ELSEVIER

Journal of Alloys and Compounds 408–412 (2006) 71–75

Journal of ALLOYS AND COMPOUNDS

www.elsevier.com/locate/jallcom

XAFS analysis of molten rare-earth-alkali metal fluoride systems

S. Watanabe [a,*], A.K. Adya [b], Y. Okamoto [c], N. Umesaki [d], T. Honma [d], H. Deguchi [e], M. Horiuchi [f], T. Yamamoto [g], S. Noguchi [h], K. Takase [i], A. Kajinami [j], T. Sakamoto [a], M. Hatcho [a], N. Kitamura [a], H. Akatsuka [a], H. Matsuura [a]

[a] *Research Laboratory for Nuclear Reactors, Tokyo Institute of Technology, 2-12-1 Meguro-ku, Tokyo 152-8550, Japan*
[b] *School of Contemporary Sciences, University of Abertay Dundee, Bell Street, Dundee DD1 1HG, UK*
[c] *Department of Materials Science, Japan Atomic Energy Research Institute, Tokai, Ibaraki 319-1195, Japan*
[d] *Japan Synchrotron Radiation Research Institute, Mikazuki, Hyogo 679-5198, Japan*
[e] *Power Engineering RandD Center, Kansai Electric Power Co. Inc., Nakoji, Amagasaki, Hyogo 661-0974, Japan*
[f] *Engineering Section, Kanden Kakou Co. Ltd., 1-2-1-1800 Benten, Minato-ku, Osaka 552-0007, Japan*
[g] *Central Research Institute of Electric Power Industry, 2-6-1 Nagasaka, Yokosuka, Kanagawa 240-0196, Japan*
[h] *Electric Power Engineering Systems Co. Ltd., 2-11-1 Iwadokita, Komae, Tokyo 201-8511, Japan*
[i] *Graduate School of Science and Technology, Niigata University, Ikarashi-Ninocho, Niigata 950-2181, Japan*
[j] *Department of Chemical Science and Engineering, Faculty of Engineering, Kobe University, Rokko-dai, Nada-ku, Kobe 657-8501, Japan*

Available online 15 June 2005

Abstract

X-ray absorption fine structure (XAFS) measurements on rare-earth-alkali metal fluoride systems (0.2 LnF_3–0.8 MF: Ln = La, Ce, Nd, Sm; M = Li, Na, K) have been carried out at 300 and 1173 K. The local structures around rare-earth-ions in both the solid and liquid phases were evaluated by the curve-fitting analysis, involving anharmonic oscillation effects at the higher temperature. This study revealed that the nearest-neighbour Ln^{3+}–F^- distance and the corresponding coordination number of F^- around Ln^{3+} in the molten state mainly depend on the lanthanide species rather than the size of the alkali metal ion.

Keywords: Molten salt; EXAFS; Local structure; Rare-earth fluoride; Pyrochemical reprocessing

1. Introduction

Molten rare-earth fluorides play important roles for various engineering applications, such as the synthesis of metal alloys, the recycling of metals, etc. We have proposed molten alkali metal fluorides as melt baths for the pyrochemical reprocessing of nuclear fuels, and investigated the structural characteristics of some molten fluorides [1]. Although, the local structures of molten chlorides have been systematically investigated in the past by using many different experimental [2] and numerical [3] approaches, the structural characteristics of molten fluorides remain experimentally unexplored so far. This is probably due to the high corrosiveness of these materials. In order to develop the pyrochemical process by using molten fluoride baths, structural information of these molten salts must first be elucidated systematically.

In this study, the local structures of molten lanthanide-alkali metal fluoride systems (0.2 LnF_3–0.8 MF: Ln = La, Ce, Nd, Sm; M = Li, Na, K) around lanthanide ions have been investigated at the room temperature and at a higher temperature above their melting points, by X-ray absorption fine structure (XAFS) spectroscopy. The resulting structural parameters between the Ln^{3+} ion and the nearest-neighbouring F^- ions are reported.

2. Experimental

Both the rare-earth fluorides, LnF_3, and the alkali metal fluorides, MF (Soekawa Co. 4N, $x LnF_3 = 0.2$), were melted in a glassy carbon crucible at 1173 K and known amounts

* Corresponding author. Tel.: +81 3 5734 3057; fax: +81 3 5734 3057.
E-mail address: souwata@nr.titech.ac.jp (S. Watanabe).

0925-8388/$ – see front matter © 2005 Elsevier B.V. All rights reserved.
doi:10.1016/j.jallcom.2005.04.105

Table 1
Experimental conditions

Facility	Beamline	Monochromator	Sample	X-ray absorption edge
SPring-8 8 GeV, 100 mA	BL16B2	Si (3 1 1) double crystal	LaF_3, LaF_3–MF	La–K (38.925 keV)
			SmF_3, SmF_3–LiF	Sm–K (46.834 keV)
	BL38B1	Si (3 1 1) double crystal	CeF_3, CeF_3–MF	Ce–K (40.443 keV)
			SmF_3–NaF, SmF_3–KF	Sm–K (46.814 keV)
PF, KEK 2.5 GeV, 400–250 mA	BL7C	Si (1 1 1) double crystal	NdF_3, NdF_3–MF	Nd–Lm (6.208 keV)
			SmF_3, SmF_3–MF	Sm–L_m (6.716 keV)

of these salts were homogeneously dispersed in dried boron nitride (BN) powder in order to obtain the best X-ray absorption spectra. The chemical reactions of the reagents with the glassy carbon crucible have not been confirmed in several heating–cooling tests. These powders were pressed into pellets of ca. 13 mm diameter and 1 mm width. Above the melting points of these salts, the BN matrix could finely keep the droplets of liquid salts dispersed inside. For each sample, a pellet was installed in an electric furnace located between the ionization chambers and the furnace was heated from 300 to 1173 K. The experimental conditions for the transmission EXAFS step-scan measurements are listed in Table 1.

3. Results and discussion

Experimental data were analysed by using WinXAS Version 2.3 [4]. In particular, the EXAFS oscillation $\chi(k)$, as a function of the photoelectron wave number k, was extracted from the normalised X-ray absorption spectrum by assuming the X-ray absorption of single atom and using combinations of second degree polynomials. The Radial Structure Function (RSF: $|\mathrm{FT}(\chi(k)k^3)|$) was obtained by Fourier transformation of k^3 weighted $\chi(k)$ spectrum in the range $k > 2.5$ Å^{-1}. The local structural parameters of the nearest-neighboring F^- ions around a Ln^{3+} ion were evaluated by the curve-fitting analysis of the predominant Ln–F correlation peak in the RSF according to,

$$\chi(k) = S_0^2 \frac{N_{\mathrm{LnF}} F(k)}{kR_{\mathrm{LnF}}^2} \exp\left(-2\sigma^2 k^2 + \frac{2}{3}C_4 k^4\right) \times \sin\left(2kR_{\mathrm{LnF}} + \delta(k) - \frac{4}{3}C_3 k^3\right), \quad (1)$$

where S_0^2, fixed as 1.0 in this study, is the probability of single-electron excitation. N_{LnF} is the coordination number of F^- at a distance R_{LnF} from Ln^{3+} and σ^2 is the Debye Waller factor, which reflects thermal and structural disorder. C_3 and C_4 are the third and fourth cumulants, respectively, which represent anharmonic oscillation effects at the high temperature. $F(k)$ and $\delta(k)$ are the backscattering amplitude and phase shift of the photoelectron, respectively, and these were calculated by using the FEFF8.0 code [5].

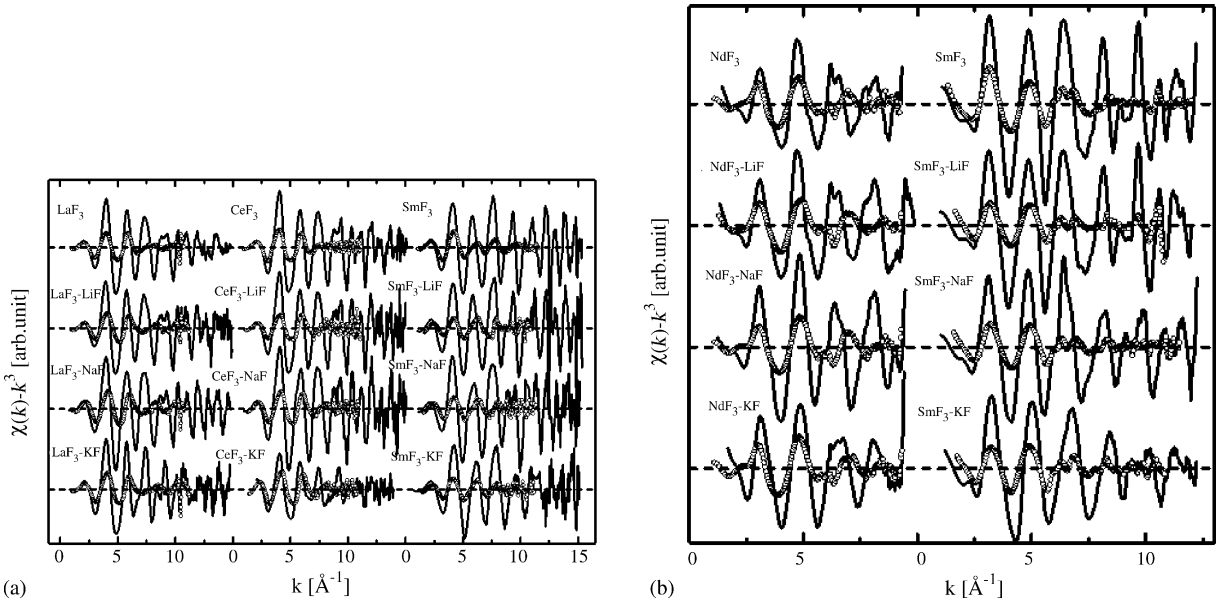

Fig. 1. EXAFS oscillations $\chi(k)k^3$ obtained by: (a) Ln–K and (b) Ln–L_{III} X-ray absorption edge spectra. Solid lines and circles correspond to measurements at 300 and 1173 K, respectively.

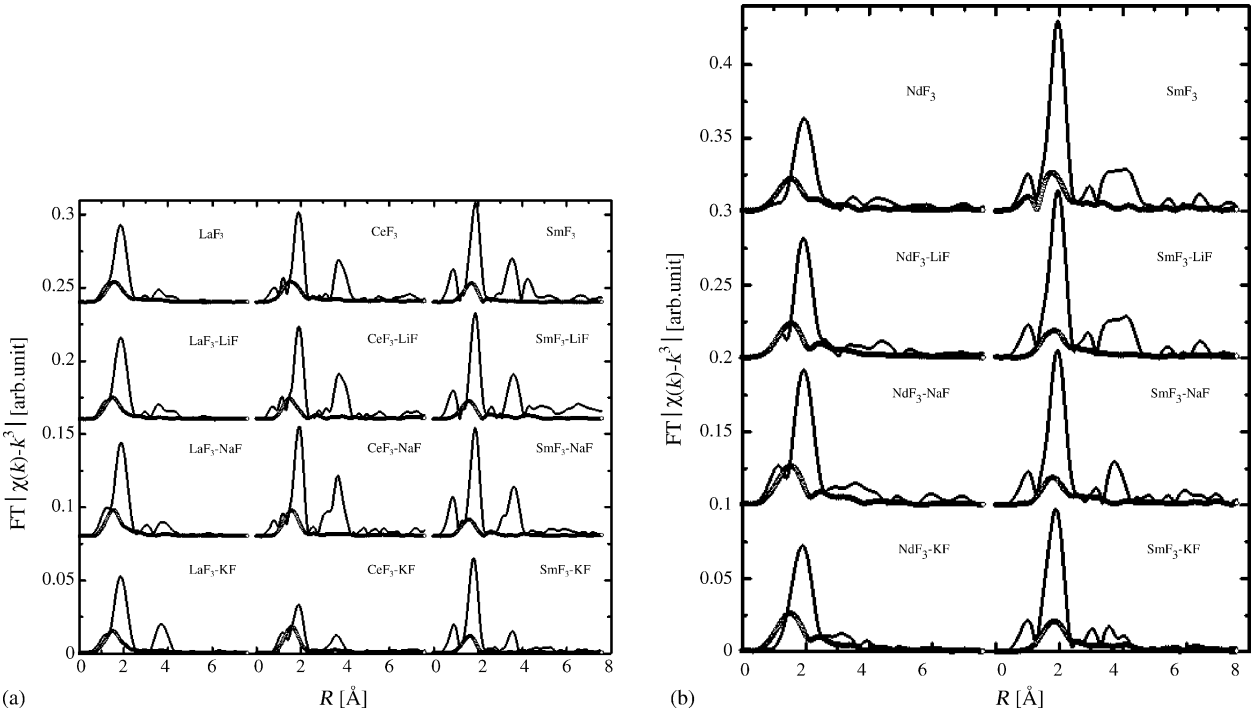

Fig. 2. RSFs $|FT(\chi(k)k^3)|$ obtained by: (a) Ln–K and (b) Ln–L_{III} X-ray absorption edge spectra. Solid lines and circles correspond to measurements at 300 and 1173 K, respectively.

EXAFS oscillations, $\chi(k)k^3$, obtained from the Ln K and L_{III} X-ray absorption spectra are shown in Fig. 1(a and b), respectively. Spectra of the mixtures at 1173 K show the EXAFS oscillations in the liquid state, while the spectra at 300 K are in the solid state.

The RSFs $|FT(\chi(k)k^3)|$ obtained from the Ln K and L_{III} X-ray absorption spectra are shown in Fig. 2(a and b), respectively. The curve-fitting analysis was carried out on a predominant peak of the RSF at ca. $R = 2$ Å, which is considered to be the Ln^{3+}–F^- nearest-neighbour distance. Structural parameters obtained by the curve-fitting procedure are listed in Table 2. At 300 K, we chose $C_3 = C_4 = 0$ (see Eq. (1)) for the curve fitting because the anharmonic vibration effects can be considered negligible at room temperature.

R_{LnF} and N_{LnF} at 300 K were evaluated as average values of the first coordination shell around Ln^{3+} ion. For instance, in the case of the pure LaF_3 crystal at the room temperature, nine F atoms surround asymmetrically a La atom within the range $2.417 < R_{LaF}$ (Å) < 2.640, and the average value of R_{LaF} is ca. 2.490 Å [6]. A comparison of these values with both the evaluated, N_{LaF} and R_{LaF}, values at 300 K listed in Table 2 shows that the current values are slightly underestimated by a few percent. This underestimation may be caused by the fact that the EXAFS signal is not sensitive to farther atoms when the atomic geometry around the X-ray absorption atom is asymmetric. Although F^- ions coordinate randomly around a Ln^{3+} ion in the liquid phase, the F^- ion arrangement becomes more symmetric than in the crystal phase upon melting. Therefore, the coordination number in the molten state might be viewed as the average number of F^- ions around the Ln^{3+} ion in various clusters, LnF_n, which may exist in the liquid, but without the underestimation caused by the asymmetric structure.

Both the inter-ionic distance, R_{LnF}, and the coordination number, N_{LnF}, of the molten salts do not change drastically on varying the alkali metal, and these values seem to depend mainly on the lanthanide ion species; LaF_3 system: $R_{LaF} = 2.42$–2.43 Å, $N_{LaF} = 5.7$–6.7, CeF_3 system: $R_{CeF} = 2.42$ Å, $N_{CeF} = 5.9$–6.9, NdF_3 system: $R_{NdF} = 2.39$–2.40 Å, $N_{NdF} = 6.7$–6.9, SmF_3 system: $R_{SmF} = 2.35$ Å, $N_{SmF} = 3.9$–4.6. While the inter-ionic distance apparently changes according to the ionic radius, $r_{Ln^{3+}}$, of the Ln^{3+} ion ($r_{La^{3+}} = 1.356$ Å, $r_{Ce^{3+}} = 1.336$ Å, $r_{Nd^{3+}} = 1.303$ Å, $r_{Sm^{3+}} = 1.272$ Å, calculated for the nine-coordinated crystals [7]), the coordination numbers, N_{LnF}, values are almost the same except for the SmF_3 system, which shows some dependence on the nature of the alkali metal species. Roughly speaking, the LaF_3, CeF_3 and NdF_3 systems are six-coordinated and SmF_3 system is four-coordinated. Thus, it is reasonable to suggest that the main factor that dominates the local structure around a given Ln^{3+} ion is the Ln^{3+}–F^- interaction due to its strong coulombic attraction. Also, the structural difference observed between the SmF_3 system and the other systems arises from the difference in the Ln^{3+}–F^- interactions resulting from the structural differences in the LnF_3 crystals at the room temperature (LaF_3, CeF_3 and NdF_3: tysonite; SmF_3: orthorhombic [6]).

Table 2
The nearest-neighbouring Ln–F structural parameters obtained by the curve-fitting analysis described in the text (see Section 3)

Edge	Sample	T (K)	N_{LnF}	R_{LnF} (Å)	σ^2 (10^{-2} Å^2)	C_3 (10^{-3} Å^3)	C_4 (10^{-4} Å^4)	Residual (%)
La–K	LaF_3	300	8.60 ± 0.17	2.45 ± 0.00	1.02 ± 0.04	0 (fix)	0 (fix)	0.77
		1173	8.08 ± 0.31	2.45 ± 0.02	3.55 ± 0.11	3.25 ± 0.67	3.89 ± 0.40	9.53
	LaF_3–LiF	300	8.83 ± 0.19	2.45 ± 0.00	0.99 ± 0.05	0 (fix)	0 (fix)	1.04
		1173	5.74 ± 0.30	2.42 ± 0.00	2.63 ± 0.07	4.17 ± 0.79	1.56 ± 0.48	6.65
	LaF_3–NaF	300	9.86 ± 0.19	2.46 ± 0.00	0.94 ± 0.07	0 (fix)	0 (fix)	1.70
		1173	6.69 ± 0.40	2.43 ± 0.01	2.56 ± 0.10	4.35 ± 0.60	1.97 ± 0.44	5.38
	LaF_3–KF	300	8.33 ± 0.10	2.45 ± 0.01	0.96 ± 0.08	0 (fix)	0 (fix)	4.33
		1173	6.18 ± 0.47	2.42 ± 0.00	2.68 ± 0.13	4.28 ± 0.61	1.31 ± 0.32	5.34
Ce–K	CeF_3	300	8.52 ± 0.17	2.42 ± 0.01	0.82 ± 0.06	0 (fix)	0 (fix)	4.71
		1173	7.93 ± 0.36	2.42 ± 0.02	3.02 ± 0.04	3.09 ± 0.21	1.35 ± 0.40	9.90
	CeF_3–LiF	300	8.91 ± 0.17	2.43 ± 0.02	0.85 ± 0.07	0 (fix)	0 (fix)	4.08
		1173	5.88 ± 0.35	2.41 ± 0.00	2.78 ± 0.10	2.95 ± 0.20	2.68 ± 0.32	8.15
	CeF_3–NaF	300	10.34 ± 0.12	2.43 ± 0.00	0.83 ± 0.09	0 (fix)	0 (fix)	2.73
		1173	6.90 ± 0.11	2.42 ± 0.01	2.49 ± 0.03	3.56 ± 0.15	1.09 ± 0.23	7.16
	CeF_3–KF	300	6.93 ± 0.08	2.42 ± 0.01	1.31 ± 0.05	0 (fix)	0 (fix)	6.03
		1173	6.91 ± 0.11	2.42 ± 0.00	2.49 ± 0.02	3.78 ± 0.11	1.45 ± 0.38	6.27
Sm–K	SmF_3	300	8.92 ± 0.03	2.38 ± 0.00	0.68 ± 0.00	0 (fix)	0 (fix)	2.98
		1173	7.42 ± 0.27	2.35 ± 0.01	3.42 ± 0.03	1.26 ± 0.38	5.19 ± 0.38	9.96
	SmF_3–LiF	300	9.12 ± 0.01	2.37 ± 0.00	0.69 ± 0.01	0 (fix)	0 (fix)	5.84
		1173	4.56 ± 0.18	2.35 ± 0.01	2.12 ± 0.03	2.67 ± 0.16	1.14 ± 0.16	8.83
	SmF_3–NaF	300	8.72 ± 0.02	2.36 ± 0.01	0.65 ± 0.01	0 (fix)	0 (fix)	5.71
		1173	3.90 ± 0.07	2.35 ± 0.01	1.92 ± 0.03	3.09 ± 0.21	0.54 ± 0.10	7.82
	SmF_3–KF	300	7.32 ± 0.12	2.30 ± 0.00	0.69 ± 0.01	0 (fix)	0 (fix)	3.47
		1173	4.48 ± 0.45	2.35 ± 0.01	2.23 ± 0.16	2.23 ± 0.30	1.52 ± 0.42	8.57
ND–L_{III}	NdF_3	300	6.24 ± 0.36	2.41 ± 0.00	1.05 ± 0.06	0 (fix)	0 (fix)	2.32
		1173	6.23 ± 0.22	2.40 ± 0.00	3.45 ± 0.05	6.25 ± 0.40	3.79 ± 0.53	9.02
	NdF_3–LiF	300	7.22 ± 0.50	2.40 ± 0.00	0.98 ± 0.08	0 (fix)	0 (fix)	6.69
		1173	6.79 ± 0.21	2.39 ± 0.00	3.55 ± 0.06	6.87 ± 0.37	4.37 ± 0.52	10.81
	NdF_3–NaF	300	8.13 ± 0.16	2.40 ± 0.00	0.92 ± 0.03	0 (fix)	0 (fix)	3.31
		1173	6.72 ± 0.37	2.40 ± 0.00	3.21 ± 0.07	6.74 ± 0.21	4.00 ± 0.39	11.13
	NdF_3–KF	300	6.93 ± 0.13	2.37 ± 0.01	1.04 ± 0.02	0 (fix)	0 (fix)	2.67
		1173	6.92 ± 0.20	2.40 ± 0.00	3.16 ± 0.06	6.65 ± 0.31	2.46 ± 0.42	8.80
Sm–L_{III}	SmF_3	300	8.72 ± 0.15	2.36 ± 0.01	0.72 ± 0.01	0 (fix)	0 (fix)	3.18
		1173	7.74 ± 0.05	2.36 ± 0.00	3.57 ± 0.02	1.26 ± 0.33	4.36 ± 0.27	7.58
	SmF_3–LiF	300	8.94 ± 0.14	2.37 ± 0.00	0.90 ± 0.03	0 (fix)	0 (fix)	3.19
		1173	4.53 ± 0.07	2.35 ± 0.01	2.85 ± 0.01	1.21 ± 0.18	1.23 ± 0.25	4.41
	SmF_3–NaF	300	8.83 ± 0.09	2.37 ± 0.00	0.98 ± 0.02	0 (fix)	0 (fix)	2.28
		1173	4.59 ± 0.06	2.35 ± 0.01	2.72 ± 0.01	1.67 ± 0.26	1.36 ± 0.21	3.12
	SmF_3–KF	300	7.60 ± 0.17	2.29 ± 0.00	0.96 ± 0.02	0 (fix)	0 (fix)	4.41
		1173	4.79 ± 0.05	2.35 ± 0.01	2.49 ± 0.02	1.00 ± 0.17	0.51 ± 0.28	5.62

Residual is defined by the equation, residual (%) = $100 \sum_{i=1} \left|\chi_{exp}(i) - \chi_{cal}(i)\right| / \sum_i \left|\chi_{exp}(i)\right|$, and the subscripts exp and cal correspond to experimental and calculation, respectively.

4. Conclusions

XAFS analysis of molten 0.2 LnF_3–0.8 MF systems (Ln = La, Ce, Nd, Sm; M = Li, Na, K) revealed that the local structure around Ln^{3+} ion in these molten salts mainly depend on the size of the Ln^{3+} ion and changing the alkali metal ion hardly affects the structural parameters. However, structural analyses of other molten fluoride systems must be carried out for a systematic and in-depth investigation on fluoride melts. The local structure around a lanthanide ion in molten alkali metal fluoride bath is expected to be different and dependent on the lanthanide fluoride crystal structure at the room temperature.

Acknowledgements

We wish to thank Dr. M. Matsuzaki of the Tokyo Institute of Technology for his technical assistance. These experiments were carried out with the approval of the Photon Factory Program Advisory Committee (Proposal No. 2002G281) and SPring-8 (Proposal No. C04A16B2-4050-N and 2004A0546-NXa-np).

References

[1] S. Watanabe, R. Toyoyoshi, T. Sakamoto, Y. Okamoto, Y. Iwadate, H. Akatsuka, H. Matsuura, J. Phys. Chem. Solids 66 (2005) 402.

[2] e.g., Y. Okamoto, H. Shiwaku, T. Yaita, H. Narita, H. Tanida, J. Mol. Struct. 641 (2002) 71.
[3] e.g., Y. Okamoto, F. Kobayashi, T. Ogawa, J. Alloys Compd. 217–273 (1998) 355.
[4] T. Ressler, J. Phys., IV 7 (1997) C2.
[5] S.I. Zabinsky, J.J. Rehr, A. Ankudinov, R.C. Albers, M.J. Eller, Phys. Rev. B. 52 (1995) 2995.
[6] R.W.G. Wyckoff, Crystal Structures, vol. 2, second ed., Interscience Publishers, 1964.
[7] R.D. Shannon, Acta Cryst. A32 (1976) 751.